



ChemComm

**The capricious nature of iodine catenation in I₂ excess,
perovskite-derived hybrid Pt(IV) compounds**

Journal:	<i>ChemComm</i>
Manuscript ID	CC-COM-09-2018-007536.R1
Article Type:	Communication

SCHOLARONE™
Manuscripts

Cite this: DOI: 10.1039/xxxxxxxxxx

The capricious nature of iodine catenation in I₂ excess, perovskite-derived hybrid Pt(IV) compounds

Hayden A. Evans,^{ab} Jessica L. Andrews,^a Douglas H. Fabini,^{bc‡} Molliegh B. Preefer,^{ab} Guang Wu,^a Anthony K. Cheetham,^{bd} Fred Wudl,^c and Ram Seshadri^{abc}

Received Date

Accepted Date

DOI: 10.1039/xxxxxxxxxx

www.rsc.org/journalname

Perovskite-derived hybrid platinum iodides with the general formula A₂Pt^{IV}I₆ (A = formamidinium FA and guanidinium GUA) accommodate excess I₂ to yield hydrogen-bond-stabilized compounds where the I₂ forms catenates with I⁻ anions on the PtI₆ octahedra.

The bonding of atoms of the same element into a series — the phenomenon of catenation — is commonly associated with certain second and third period main group elements such as boron, carbon, sulfur, and phosphorous. This tendency is governed by multiple factors including mean bond-dissociation energy, sterics, electronegativity, and orbital hybridization.[?] Generally, catenation occurs less frequently as one moves down the periodic table as orbitals grow more diffuse and bonding strength decreases. An exception would be catenated iodides (commonly referred to as polyiodides, although the term oligoiodide is perhaps more appropriate), which are numerous and demonstrate great diversity in length as well as in structure. At this time, the Cambridge Crystallographic Data Center (CCDC) lists approximately 1600 structures containing some form of an I–I linkage with three or more I atoms. Examples of solid-state oligoiodide materials include molecular salts where triiodide (I₃⁻) subunits are charge balanced by counter cations, and connected frameworks where many oligoiodide moieties (I₂, I₃⁻, I₅⁻, I₇⁻, I₉⁻, etc) link together.^{??}

Recently, some of us reported the crystallographic structure of a rare iodine homopolymer in a pyrroloperylene-iodide compound, reminiscent of the elusive starch-iodine complex.[?] The variety of oligoiodide structures results from favorable donor-acceptor interactions, and the many cations, anions, and solvent molecules that appear to impact these interactions in the solid state.

Donor-acceptor properties of iodine find many applications, including for increasing the conductivity of organic metals and conducting polymers,[?] enhancing the efficiency of dye-sensitized solar cells,^{??} and improving the photocatalysis of materials for hydrogen evolution.^{??} Recent interest in iodide-based perovskite photovoltaic materials^{???} has engendered reports of incorporating I₃⁻ subunits into a hybrid bismuth iodide compound in order to introduce intergap electronic states that red-shifted the band gap.[?] This result is interesting in light of most Bi–I solar energy materials displaying relatively large bandgaps regardless of structure.[?] Materials that contained neutral I₂ molecules linking discrete [BiI₆]³⁻ octahedra have also been noted to display direct bandgaps of ≈1.3 eV.[?] However, it was stated that covalency between the I₂ and [BiI₆]³⁻ iodides did not appear to be present, and the structure should not be viewed as a [BiI₆]³⁻–I₂–[BiI₆]³⁻ 1D chain. This suggests that simple iodine/iodide proximity, not covalency, was enough to induce favorable properties of these materials in the solid state.

Here we present the findings that the hydrogen-bonded framework perovskite-derived materials, (FA)₂PtI₆ and (GUA)₂PtI₆ (FA = formamidinium and GUA = guanidinium), which were recently studied as members of an A₂PtI₆ series,[?] can be recrystallized as excess I₂ containing compounds. The new compounds, (FA)₂PtI₆•2I₂ and (GUA)₈(PtI₆)₃[PtI₄(I₃)₂]•2I₂, are described herein. In order to understand how size and hydrogen bonding tendencies impact the formation of these oligoiodide materials, a dimethylammonium (DMA) Pt–I compound was also prepared and studied. The solid (DMA)₃PtI₆(I₃) provides valuable insight into how hydrogen bonding is essential to stabilizing this class of halide structures. Interestingly, all three materials,

^aDepartment of Chemistry and Biochemistry, University of California Santa Barbara, California 93106 United States. E-mail: seshadri@mrl.ucsb.edu

^bMaterials Research Laboratory, University of California Santa Barbara, California 93106 United States

^cMaterials Department, University of California Santa Barbara, California 93106 United States

^dDepartment of Materials Science and Engineering, National University of Singapore, Singapore 117575, Singapore

[‡]Present address: Department of Nanochemistry, Max Planck Institute for Solid State Research, Heisenbergstr. 1, 70569 Stuttgart, Germany

[†] Electronic Supplementary Information (ESI) available. This includes experimental details, crystallographic files (CCDC 1864903–1864907), structure descriptions, PXRD, TGA, DSC, and band structure information]. See DOI: 10.1039/b000000x/

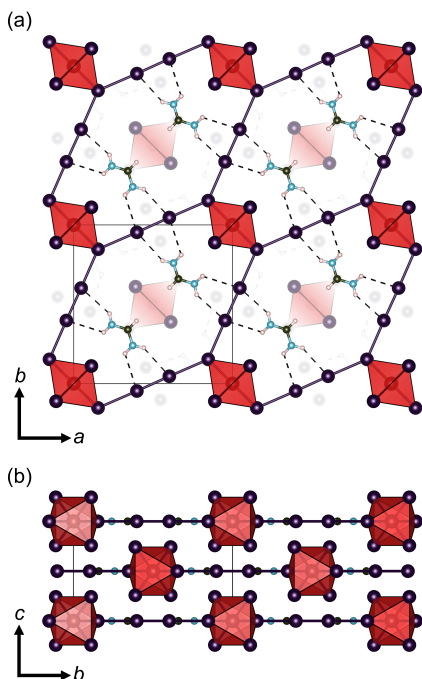


Fig. 1 Crystal structure of $(\text{FA})_2\text{PtI}_6 \cdot 2\text{I}_2$ at 100 K. Atom color key; Pt = Red, I = purple, N = blue, C = black, H = white. (a) Depiction of the 1D chains forming between the iodides on the $[\text{PtI}_6]^{2-}$ octahedra and I_2 molecules. Hydrogen bonding columns that form between the FA cations and the I_2 molecules are displayed with dashed lines. The pertinent bond lengths are: I_2 molecule 2.77 Å; $\text{I}_2\text{-I}^-$ 3.30 Å; $\text{N-H}\cdots\text{I}_2$ 3.0 Å. (b) Side view of the 2D sheets that are found parallel to the ab plane.

despite their distinct dimensionalities, display similar optical absorption profiles.

The structures of the hybrid platinum poly/oligoiodide materials, $(\text{FA})_2\text{PtI}_6 \cdot 2\text{I}_2$, $(\text{GUA})_8(\text{PtI}_6)_3[\text{PtI}_4(\text{I}_3)_2] \cdot 2\text{I}_2$, and $(\text{DMA})_3\text{PtI}_6(\text{I}_3)$, are presented in Figures ?? and ?. Figure ?? (a) emphasizes the intriguing 1D polyiodide chains that form in $(\text{FA})_2\text{PtI}_6 \cdot 2\text{I}_2$ between apical iodides of the $[\text{PtI}_6]^{2-}$ octahedra and the I_2 molecules, as well as the 1D hydrogen bonding columns that form between the FA cations and the same I_2 molecules. Figure ?? (b) depicts the sheet-like structure formed by the $\text{I}_2\text{-}[\text{PtI}_6]^{2-}$ chains and the columns of FA cations and I_2 molecules. Compounds which present I_2 molecules or polyiodide moieties in donor-acceptor interactions with metal halide octahedra, similar to the aforementioned $\text{I}_2\text{-}[\text{BiI}_6]^{3-}$ system, are fairly common, ??? but the infinite 1D $\text{I}_2\text{-I-I}_2$ chain that extends through the structure of $(\text{FA})_2\text{PtI}_6 \cdot 2\text{I}_2$ is to our knowledge the first example reported with such short distances between atoms.[?] By convention, covalent bonds between iodine/iodide atoms should have an interatom distance of no greater than 3.30 Å.[?] At 300 K, the single crystal X-ray diffraction measured distance of the $\text{I}_2\text{-I}^-$ bond in $(\text{FA})_2\text{PtI}_6 \cdot 2\text{I}_2$ is 3.32 Å, and at 100 K it is 3.30 Å. If we adhere to the 3.30 Å cutoff, only the low temperature structure of $(\text{FA})_2\text{PtI}_6 \cdot 2\text{I}_2$ qualifies as a polyiodide material, but as we later demonstrate via Raman spectroscopy, this material displays vibrations indicative of a polyiodide material at 300 K. Furthermore, at both 300 K and 100 K, the I_2 intermolecular bond lengths are longer than the known solid-state I_2 bond distance of

2.67 Å (2.75 Å and 2.77 Å, respectively) suggesting that between 300 K and 100 K the donor apical iodides of the $[\text{PtI}_6]^{2-}$ octahedra are decreasing the $\text{I}_2\text{-I-I}_2$ bond order. This is in agreement with a molecular orbital (MO) description of this compound,[?] which shows that the highest occupied molecular orbital (HOMO) has some degree of antibonding character.

Additionally, we note the significance of certain characteristics of the FA cations in $(\text{FA})_2\text{PtI}_6 \cdot 2\text{I}_2$. Firstly, they are ordered, which is unlike the "tumbling" FA and methylammonium cations in APbI₃ perovskites.^{????} Secondly, they hydrogen bond explicitly with the I_2 molecules and not the $[\text{PtI}_6]^{2-}$ iodides, as seen in the parent compound, $(\text{FA})_2\text{PtI}_6$. If one considers both the FA cation arrangement, and the I_2 molecules location relative to the apical iodides on the $[\text{PtI}_6]^{2-}$ octahedra, one can see that these are potential structural signatures of halogen bonding.[?] In halogen bonding, covalently bonded, easily polarizable halogen atoms (like iodine) can form nucleophilic (negative) and electrophilic (positive) sides, with the electrophilic side being denoted as the "σ-hole." We have calculated the electron localization function (ELF) and electrostatic potential for $(\text{FA})_2\text{PtI}_6 \cdot 2\text{I}_2$, and discuss the results in the last section of this work, as well as in the ESI.†

Figure ?? (a) shows the structure of $(\text{GUA})_8(\text{PtI}_6)_3[\text{PtI}_4(\text{I}_3)_2] \cdot 2\text{I}_2$ with organic cations omitted for clarity emphasizing the observed secondary $\text{I}\cdots\text{I}$ bonding network (see ESI† for Figures with organic cation locations). Secondary $\text{I}\cdots\text{I}$ bonds are interactions that are often seen in oligoiodide networks, and occur at distances between the previously mentioned cutoff for I-I covalent bonds, 3.30 Å, and the $\text{I}\cdots\text{I}$ van der Waals distance, 3.9 Å.[?] In $(\text{GUA})_8(\text{PtI}_6)_3[\text{PtI}_4(\text{I}_3)_2] \cdot 2\text{I}_2$ there are three crystallographically independent Pt sites, each with distinct local environments. These three Pt octahedral environments are denoted in Figure ?? (a) and (b) with differing colors as well as bolded numbers (1–3) which coincide with the .cif file Pt label assignments. **1** refers to the $[\text{PtI}_6]^{2-}$ octahedra that have no close $\text{I}\cdots\text{I}$ secondary bonding associations, **2** to the $[\text{PtI}_6]^{2-}$ octahedra that have two close secondary $\text{I}\cdots\text{I}$ bonding associations with I_3 ligands of the $[\text{PtI}_4(\text{I}_3)_2]^{2-}$ moieties, and **3**, which refers to the $[\text{PtI}_4(\text{I}_3)_2]^{2-}$ moieties. The species **3**, in addition to forming secondary $\text{I}\cdots\text{I}$ bonding associations with **2**, also forms secondary bonds with I_2 molecules in the ab -plane.† Figure ?? (b) illustrates one such secondary-bonding chain that forms between **3** and **2**, with bond lengths of the I_3 subunit (3.12 Å and 2.80 Å) from species **3** denoted. The occurrence of **3** is quite interesting, because to our knowledge, no similar Pt or other metal based moiety has been reported to date. The labeled bond lengths are reminiscent of other asymmetric I_3^- anion bonds [2.7(1) Å and 3.2(1)],[?] and, as we demonstrate below, the Raman spectrum displays signatures of the I_3 subunit. As to the GUA cations, they form a complex and extensive hydrogen bonding network almost exclusively with $[\text{PtI}_6]^{2-}$ octahedra iodides.† Each of the four crystallographically independent GUA cations connect **1**, **2**, and **3** together, each in a distinct way, but with uncanny similarity to the GUA cations in its parent compound, $(\text{GUA})_2\text{PtI}_6$.† This suggests that in addition to the secondary iodide network, the hydrogen bonding network is a considerable structural stabilizer.

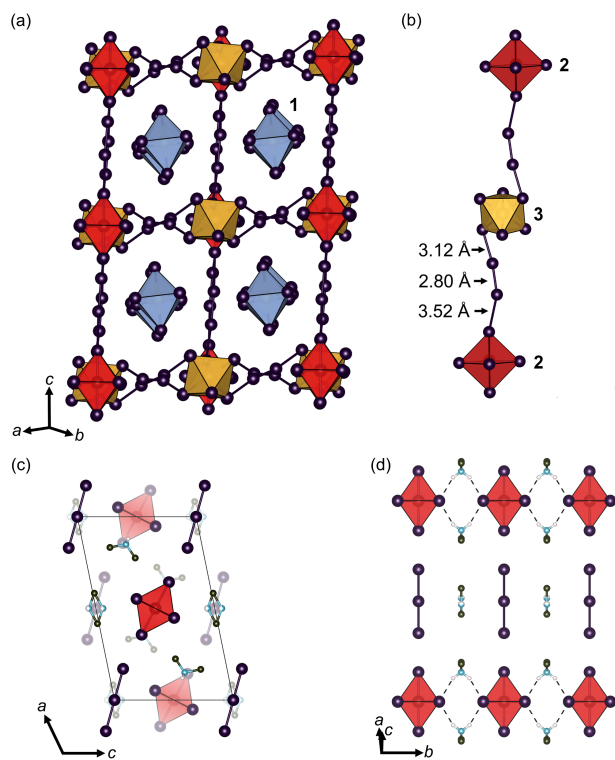


Fig. 2 The crystal structures of [(a) and (b)] $(\text{GUA})_8(\text{PtI}_6)_3[\text{PtI}_4(\text{I}_3)_2]\cdot 2\text{I}_2$ and [(c) and (d)] $(\text{DMA})_3\text{PtI}_6(\text{I}_3)$ at 100 K. Atom color key; I = purple, N = blue, C = black, H = white. (a) View of the $(\text{GUA})_8(\text{PtI}_6)_3[\text{PtI}_4(\text{I}_3)_2]\cdot 2\text{I}_2$ structure with organic cations omitted for clarity, so as to better display the oligoiodide network. To signify crystallographic independence, the Pt octahedra colors are varied and labeled with bolded numbers **1-3** in the $(\text{GUA})_8(\text{PtI}_6)_3[\text{PtI}_4(\text{I}_3)_2]\cdot 2\text{I}_2$ structure. (b) View of the crystallographically observed $[\text{PtI}_4(\text{I}_3)_2]^{2-}$ moiety **3** that forms secondary bonding chains along the c -axis with $[\text{PtI}_6]^{2-}$ octahedra **2**. (c) View of $(\text{DMA})_3\text{PtI}_6(\text{I}_3)$ down the b -axis. Hydrogen atoms are included on the DMA cations that are ordered, as these cations hydrogen bond with nearby $[\text{PtI}_6]^{2-}$ octahedra. (d) View of $(\text{DMA})_3\text{PtI}_6(\text{I}_3)$ depicting the hydrogen bonding interactions between DMA cations and $[\text{PtI}_6]^{2-}$ octahedra, as well as the arrangement of I_3^- anions relative to the nearby $[\text{PtI}_6]^{2-}$ octahedra. The distance between apical $[\text{PtI}_6]^{2-}$ iodides and nearby I_3^- is 3.49 Å.

Figures ?? (c) and (d) illustrate the structure of $(\text{DMA})_3\text{PtI}_6(\text{I}_3)$, where Figure ?? (c) shows the arrangement of $[\text{PtI}_6]^{2-}$ octahedra, I_3^- moieties, as well as the two distinct types of DMA cations; one that is ordered and one that is not. Figure ?? (d) shows the hydrogen bonding of the ordered DMA, where the N–H...I hydrogen bond lengths are at a distance of 2.87 Å and N to I distances are 3.68 Å; these are considered to be medium/strong interactions based on previous neutron diffraction studies.[?] The I_3^- moieties are aligned with the $[\text{PtI}_6]^{2-}$ octahedra at a distance of 3.49 Å (secondary I...I bonding).[?] Initially, we sought to make a DMA-containing A_2PtI_6 compound to juxtapose the materials $(\text{FA})_2\text{PtI}_6$ and $(\text{GUA})_2\text{PtI}_6$. We believed this $(\text{DMA})_2\text{PtI}_6$ compound, with a cation roughly the size of FA but with less than half the hydrogen bonding sites, would better inform us as to the impact of hydrogen bonding in these halide materials. It was our intention to recrystallize this hypothetical $(\text{DMA})_2\text{PtI}_6$ compound and observe the differences in I_2 inclusion. However, the $(\text{DMA})_2\text{PtI}_6$ compound could not be isolated, and only the com-

pound, $(\text{DMA})_3\text{PtI}_6(\text{I}_3)$, formed. Though not our original intention, this raises a significant question: "Why did $(\text{DMA})_2\text{PtI}_6$ not form?" In our previous report,[?] we discussed how the substantial hydrogen bonding capacity of the FA and GUA moieties engaged as structural guides. We believe that the similar size but reduced hydrogen bonding capacity of the DMA cation (compared to the FA cation) serves as a prime example to the significance of hydrogen bonding in these lower dimensional halide materials. Namely, that without a cation that can form numerous attractive H...I interactions, the electrostatic forces between cation and anion are not sufficient to stabilize a A_2PtI_6 molecular salt.

Raman spectra illustrate the I–I bonding character of these compounds, and are presented in Figure ?? (a). Two $[\text{PtI}_6]^{2-}$ octahedron Pt–I vibrations of varying strengths can be seen at 141 cm^{-1} and 156 cm^{-1} in all samples tested.[?] The other vibrations of interest are near 125 cm^{-1} and 180 cm^{-1} , which are attributed to the vibrations of I_3^- and I_2 , respectively.[?] When classifying the polyiodide character of $(\text{FA})_2\text{PtI}_6\cdot 2\text{I}_2$, the absence of a strong I_2 vibration near 180 cm^{-1} is quite telling, as this vibration will shift to lower energies if the I_2 molecule is acting as an acceptor. The amount of shift will depend on the strength of the respective donor species.[?] It is likely that for $(\text{FA})_2\text{PtI}_6\cdot 2\text{I}_2$, the I_2 vibration has shifted to lower energies near 110 cm^{-1} , which is frequently seen in spectra of extended polyiodides.^{??} This suggests that even at room temperature (where the $\text{I}_2\text{--I}^-$ distance is slightly greater than 3.3 Å) this material is best thought of as a polyiodide. The material $(\text{GUA})_8(\text{PtI}_6)_3[\text{PtI}_4(\text{I}_3)_2]\cdot 2\text{I}_2$, which has both I_2 molecules as well as I_3^- moieties, displays an expected Raman spectrum with vibrations at both 180 cm^{-1} and 125 cm^{-1} . For $(\text{DMA})_3\text{PtI}_6(\text{I}_3)$, the expected I_3^- vibration near 125 cm^{-1} is present, in addition to a peak near 110 cm^{-1} that is seen in Raman spectra of longer chain oligoiodides,[?] and 140 cm^{-1} , which is seen in Raman spectra for symmetric I_3^- containing compounds.[?] In this respect, both $(\text{GUA})_8(\text{PtI}_6)_3[\text{PtI}_4(\text{I}_3)_2]\cdot 2\text{I}_2$ and $(\text{DMA})_3\text{PtI}_6(\text{I}_3)$ are best considered oligoiodide networks.

The optical absorption spectra of the three new poly/oligoiodide compounds, as well as their parent compounds, are presented in Figure ?? (b). We observe similar optical properties for all materials tested, as was previously observed for the A_2PtI_6 series.[?] For these platinum based compounds, the charge-transfer absorption of the $[\text{PtI}_6]^{2-}$ moieties dominates, regardless of structure. However, one clear difference is the increased absorption in the higher energy (2.5 eV – 3.75 eV) of the spectra of $(\text{FA})_2\text{PtI}_6\cdot 2\text{I}_2$ and $(\text{GUA})_8(\text{PtI}_6)_3[\text{PtI}_4(\text{I}_3)_2]\cdot 2\text{I}_2$. This increased absorption is caused by the higher-energy states of the I_2 molecules that lie above the platinum d_{eg} states. The band structure of $(\text{FA})_2\text{PtI}_6\cdot 2\text{I}_2$ displays the typical underestimation of band gap when compared with experiment.[†]

Lastly, Figure ?? (a) displays the electron localization function (ELF) around iodine atoms and ions in $(\text{FA})_2\text{PtI}_6\cdot 2\text{I}_2$, projected on the structure, on the plane that contains the infinite polyiodide chains. The lone pair lobes around the I_2 units are arranged axially along $\text{I}^-\text{--I}_2\text{--I}^-$, suggesting potential covalency in the interaction with the lone pairs on the I^- anions. Significant differences in the shape of the localization between the apical iodides of the $[\text{PtI}_6]^{2-}$ octahedra, and the four equatorial iodides not a part of

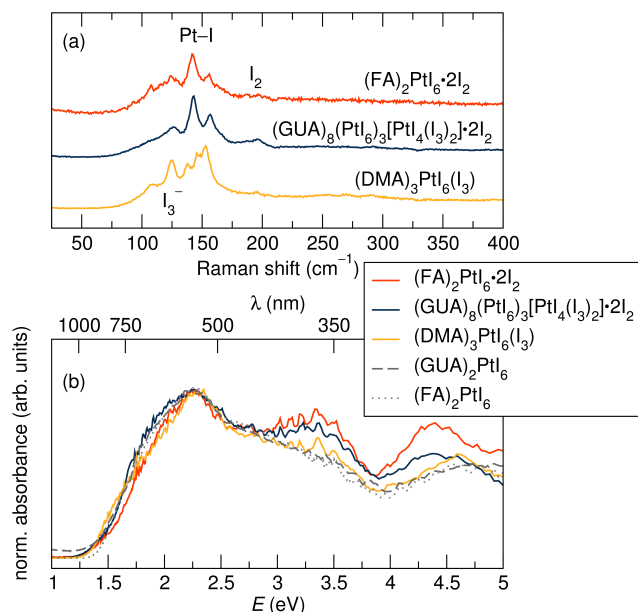


Fig. 3 (a) Raman spectra of the poly/oligoiodide materials. (b) Normalized optical absorption spectra (following Kubelka-Munk transformation of diffuse reflectance spectra) for the poly/oligoiodide materials. The spectra of the parent compounds $(\text{FA})_2\text{PtI}_6$ and $(\text{GUA})_2\text{PtI}_6$ are included for comparison.

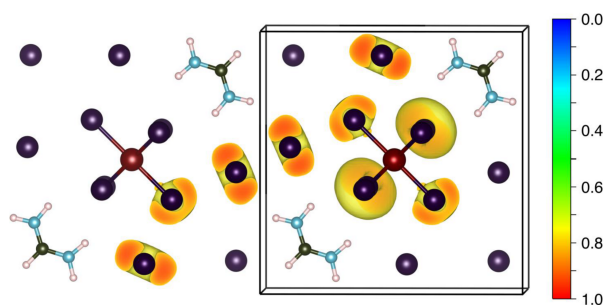


Fig. 4 Crystal structure of $(\text{FA})_2\text{PtI}_6 \bullet 2\text{I}_2$ depicted in the plane containing the infinite polyiodide chains. The ELF is displayed for an isosurface value of 0.8, showing the lone pairs around select iodide ions and I_2 moieties.

the 1D polyiodide chain, are also seen, suggesting that the apical iodides are indeed involved in some degree of bond formation within this 1D chain. Furthermore, we present the electrostatic potential for $(\text{FA})_2\text{PtI}_6 \bullet 2\text{I}_2$ in the ESI, showing subtle evidence of σ -holes on the I_2 molecules.† Given the appropriate angle and direction of the $\text{I}-\text{I} \cdots \text{I}$ and $\text{N}-\text{H} \cdots \text{I}$ bonds and the possible σ -hole, there is potential for halogen bonding stabilizing the observed structure of $(\text{FA})_2\text{PtI}_6 \bullet 2\text{I}_2$.

In conclusion, we have presented three new hybrid platinum iodide compounds that emphasize the tendency of iodine and iodide to catenate, even when the iodide is part of a complex anion. Hydrogen bonding appears to play a large role in stabilizing the observed structures.

Conflicts of interest

There are no conflicts to declare.

Acknowledgments

This work was supported by the U.S. Department of Energy, Office of Science, Basic Energy Sciences under award number DE-SC-0012541. The use of the Shared Experimental Facilities of the Materials Research Science and Engineering Center (MRSEC) at UCSB is gratefully acknowledged (NSF DMR 1720256). We additionally acknowledge the Center for Scientific Computing at UCSB (NSF CNS-1725797 and NSF DMR-1720256). DHF thanks the National Science Foundation Graduate Research Fellowship Program for support (DGE 1144085). AKC thanks the Ras al Khaimah Centre for Advanced Materials for financial support. We thank an anonymous referee for advice on halogen bonding.

Notes and references

- D. M. P. Mingos, *Essential Trends in Inorganic Chemistry*, Oxford University Press Oxford, 1998.
- P. H. Svensson and L. Kloo, *Chem. Rev.*, 2003, **103**, 1649–1684.
- S. A. Adonin, M. N. Sokolov and V. P. Fedin, *Coord. Chem. Rev.*, 2018, **367**, 1–17.
- S. Madhu, H. A. Evans, V. V. T. Doan, A. Nguyen, J. G. Labram, G. Wu, M. L. Chabinye, R. Seshadri and F. Wudl, *Angew. Chemie Int. Ed.*, 2016.
- A. J. Heeger, S. Kivelson, J. R. Schrieffer and W.-P. Su, *Rev. Mod. Phys.*, 1988, **60**, 781.
- A. Hagfeldt and M. Grätzel, *Acc. Chem. Res.*, 2000, **33**, 269–277.
- B. Li, L. Wang, B. Kang, P. Wang and Y. Qiu, *Sol. Energy Mater. Sol. Cells*, 2006, **90**, 549–573.
- E. A. Gibson, *Chem. Soc. Rev.*, 2017, **46**, 6194–6209.
- G. Zhang, M. Zhang, X. Ye, X. Qiu, S. Lin and X. Wang, *Adv. Mater.*, 2014, **26**, 805–809.
- Y. Zhao and K. Zhu, *Chem. Soc. Rev.*, 2016, **45**, 655–689.
- D. H. Fabini, J. G. Labram, A. J. Lehner, J. S. Bechtel, H. A. Evans, A. Van der Ven, F. Wudl, M. L. Chabinye and R. Seshadri, *Inorg. Chem.*, 2016, **56**, 11–25.
- B. Saparov and D. B. Mitzi, *Chem. Rev.*, 2016, **116**, 4558–4596.
- W. Zhang, X. Liu, L. Li, Z. Sun, S. Han, Z. Wu and J. Luo, *Chem. Mater.*, 2018, **30**, 4081–4088.
- A. J. Lehner, D. H. Fabini, H. A. Evans, C.-A. Hébert, S. R. Smock, J. Hu, H. Wang, J. W. Zwanziger, M. L. Chabinye and R. Seshadri, *Chem. Mater.*, 2015, **27**, 7137–7148.
- T. A. Shestimerova, N. A. Yelavik, A. V. Mironov, A. N. Kuznetsov, M. A. Bykov, A. V. Grigorieva, V. V. Utochnikova, L. S. Lepnev and A. V. Shevelkov, *Inorg. Chem.*, 2018, **57**, 4077–4087.
- H. A. Evans, D. H. Fabini, J. L. Andrews, M. Koerner, M. B. Preefer, G. Wu, F. Wudl, A. K. Cheetham and R. Seshadri, *Inorg. Chem.*, 2018, **57**, 10375–10382.
- A. N. Usoltsev, S. A. Adonin, P. A. Abramov, A. S. Novikov, V. R. Shayapov, P. E. Plyusnin, I. V. Korolkov, M. N. Sokolov and V. P. Fedin, *Eur. J. Inorg. Chem.*, 2018, **2018**, 3264–3269.
- T. A. Shestimerova, N. A. Golubev, N. A. Yelavik, M. A. Bykov, A. V. Grigorieva, Z. Wei, E. V. Dikarev and A. V. Shevelkov, *Cryst. Growth Des.*, 2018, **18**, 2572–2578.
- M. Berkei, J. F. Bickley, B. T. Heaton and A. Steiner, *Chem. Commun.*, 2002, 2180–2181.
- D. Schneider, A. Schier and H. Schmidbaur, *Dalt. Trans.*, 2004, 1995–2005.
- K. F. Purcell and J. C. Kotz, *An Introduction to Inorganic Chemistry*, Holt Rinehart & Winston, 1980.
- R. E. Wasylshen, O. Knop and J. B. Macdonald, *Solid State Commun.*, 1985, **56**, 581–582.
- A. Poglitsch and D. Weber, *J. Chem. Phys.*, 1987, **87**, 6373–6378.
- M. T. Weller, O. J. Weber, J. M. Frost and A. Walsh, *J. Phys. Chem. Lett.*, 2015, **6**, 3209–3212.
- D. H. Fabini, C. C. Stoumpos, G. Laurita, A. Kaltzoglou, A. G. Kontos, P. Falaras, M. G. Kanatzidis and R. Seshadri, *Angew. Chemie Int. Ed.*, 2016, **55**, 15392–15396.
- G. Cavallo, P. Metrangolo, R. Milani, T. Pilati, A. Priimagi, G. Resnati and G. Terreno, *Chem. Rev.*, 2016, **116**, 2478–2601.
- K. N. Robertson, T. S. Cameron and O. Knop, *Can. J. Chem.*, 1996, **74**, 1572–1591.
- T. Steiner, *Acta Crystallogr. Sect. B*, 1998, **54**, 456–463.
- H. Hamaguchi, *J. Chem. Phys.*, 1978, **69**, 569–578.
- P. Deplano, F. A. Devillanova, J. R. Ferraro, F. Isaia, V. Lippolis and M. L. Mercuri, *Appl. Spectrosc.*, 1992, **46**, 1625–1629.
- P. H. Svensson and L. Kloo, *J. Chem. Soc. Dalt. Trans.*, 2000, 2449–2455.